

Array-Based Structure and Gene Expression Relationship Study of Antitumor Sulfonamides Including *N*-[2-[(4-Hydroxyphenyl)amino]-3-pyridinyl]-4-methoxybenzenesulfonamide and *N*-(3-Chloro-7-indolyl)-1,4-benzenedisulfonamide

Takashi Owa,^{*,†} Akira Yokoi,[†] Kanami Yamazaki,[‡] Kentaro Yoshimatsu,[§] Takao Yamori,[‡] and Takeshi Nagasu[†]

Eisai Co., Ltd., 5-1-3 Tokodai, Tsukuba, Ibaraki 300-2635, Japan, and Cancer Chemotherapy Center, Japanese Foundation for Cancer Research, 1-37-1 Kami-Ikebukuro, Toshima-ku, Tokyo 170-8455, Japan

Received March 6, 2002

Compounds from sulfonamide-focused libraries have been evaluated in cell-based antitumor screens using the COMPARE analysis with a panel of 39 human cancer cell lines and flow cytometric cell cycle analysis. Thus far, **2** (*N*-[2-[(4-hydroxyphenyl)amino]-3-pyridinyl]-4-methoxybenzenesulfonamide (E7010)) and **3** (*N*-(3-chloro-7-indolyl)-1,4-benzenedisulfonamide (E7070)) have been selected from the collections as potent cell cycle inhibitors, which have progressed to clinical trials. Compound **2** is an orally active antimetabolic agent disrupting tubulin polymerization, whereas compound **3** belongs to a novel class of antiproliferative agents causing a decrease in the S phase fraction along with G1 and/or G2 accumulation in various cancer cell lines. Because both compounds exhibited preliminary clinical activities in the phase I setting, we decided to examine further this series of oncolytic small molecules, particularly by using high-density oligonucleotide microarray analysis. The array data have enabled us to characterize these two classes of antitumor sulfonamides on the basis of gene expression changes, illuminating the essential pharmacophore structure and drug-sensitive cellular pathways for each class. Moreover, the dual character of **5** (*N*-(3-chloro-7-indolyl)-4-methoxybenzenesulfonamide (ER-67880)), resembling both **2** and **3**, was revealed by array-based transcription profiling, though the **3**-type profile of this molecule had not been apparent in the cell-based phenotypic screens. These results provide an example of the utility of structure and gene expression relationship studies in medicinal genomics.

Introduction

The draft release of the human genome sequence has tremendous potential benefits for human health care.^{1,2} Substantial endeavors of translational studies “from lab to bedside” are currently in progress by means of emerging new technologies such as bioinformatics, transcriptomics (DNA microarray analysis), and proteomics. Interdisciplinary research utilizing these technologies should provide a more rational basis for drug discovery and development programs. A recent trial in the Developmental Therapeutics Program (DTP) of the National Cancer Institute (NCI) presents an advanced example in which the correlation between gene expression and drug activity patterns in the NCI60 cancer cell lines was evaluated to integrate large databases on gene expression and anticancer drug pharmacology.³ The COMPARE analysis in the DTP represents a bioinformatic approach for categorizing anticancer agents according to their antiproliferative “fingerprint” patterns against a panel of diverse human cancer cell lines.⁴ DNA microarray analysis in cancer research has allowed us to identify molecular differences between normal and cancer cells and to clarify the heterogeneity of cancer on a genome-wide scale.^{5,6} The ultimate goal of these

research efforts is considered to be personalized therapy, i.e., specifying the most effective drugs against a particular cancer in an individual patient.

The selection of the optimal treatment for each cancer patient will require precise molecular diagnosis based on gene expression profiles in cancerous tissues.^{5,6} At the same time, the drug effect on an individual target and/or its downstream markers may be used as molecular biological endpoints for pharmacodynamic assessment. Although tumor regression is a well-established endpoint, it appears urgently necessary to provide a firm molecular basis for the clinical benefit of “disease stabilization” accompanied by improvement in progression-free survival (PFS) and quality of life (QOL). A critical aspect of this problem is identifying tumor changes in gene expression relevant to drug efficacy. Array-based hybridization technology has proved to be particularly useful for this purpose in preclinical studies to date.^{7–9}

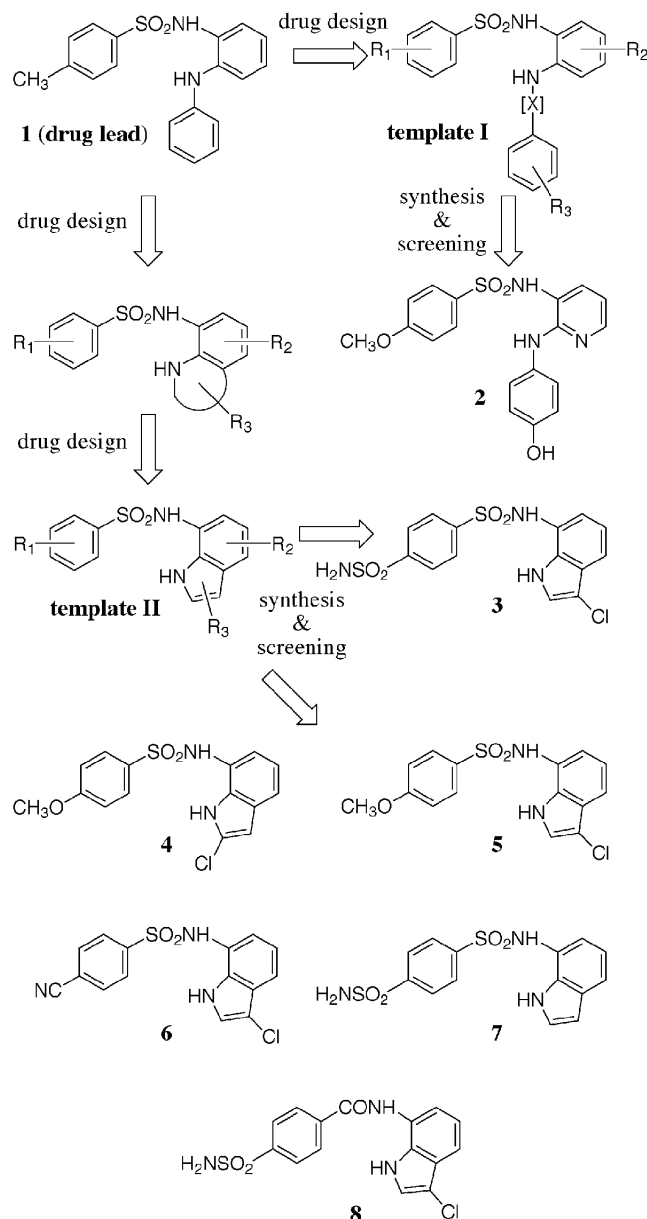
Recent trends in cancer research strongly suggest the increasing importance of accurate, systematic, and molecular mechanism-based classification of anticancer chemotherapeutics.¹⁰ In relation to this point, an integrated database of chemosensitivity to 55 anticancer drugs and gene expression profiles of 39 human cancer cell lines has been reported very recently.^{11a} There is a growing possibility that comprehensive databases will be developed further to connect antitumor activity profiles and drug-induced transcriptional changes for

* To whom correspondence should be addressed. Phone: +81-298-47-7196. Fax: +81-298-47-7614. E-mail: t-owa@hhc.eisai.co.jp.

[†] Laboratory of Seeds Finding Technology, Eisai Co., Ltd.

[‡] Japanese Foundation for Cancer Research.

[§] Discovery Research Laboratories II, Eisai Co., Ltd.

Scheme 1. Compounds from Sulfonamide-Focused Libraries

each chemotherapeutic agent. Therefore, we decided to scrutinize a series of sulfonamide antitumor agents discovered in these laboratories based on the COMPARE algorithm of the Disease-Oriented Screening (DOS) program¹¹ and Affymetrix GeneChip analysis¹² with HuGene FL (Hu6800) arrays. In this study, seven compounds selected from our sulfonamide-focused libraries (Scheme 1) were characterized in terms of the fingerprint patterns of cell growth inhibition and transcriptional alteration.

Antitumor Sulfonamides

Starting from the discovery of compound **1** as an anticancer drug lead, a large number of sulfonamide molecules have been synthesized so far using templates **I** and **II** (Scheme 1).^{13,14} Compound **2** (*N*-[2-[(4-hydroxyphenyl)amino]-3-pyridinyl]-4-methoxybenzenesulfonamide), an early drug candidate from the template **I** series, potently inhibited microtubule assembly by binding to

tubulin at the colchicine site.^{13,15} Because of its good antitumor activity in vivo against both rodent tumors and human tumor xenografts,¹⁶ **2** entered clinical trials as an orally active tubulin polymerization inhibitor. Despite the drug-related adverse effect of peripheral neuropathy, clinical activity was reported in 2 out of 16 patients in the phase I setting; spinal cord metastasis was reduced by 74% in a patient with uterine sarcoma, and a minor response was obtained in a patient with pulmonary adenocarcinoma.¹⁷

A structure–activity relationship (SAR) study based on template **II** resulted in the discovery of another novel antitumor sulfonamide **3** (*N*-(3-chloro-7-indolyl)-1,4-benzenedisulfonamide), which did not exhibit antimetabolic action.^{18,19} Following compound **3** treatment, P388 murine leukemia cells accumulated in the G1 phase but not in the M phase of the cell cycle.^{18,20} In an experiment using HCT116 human colon cancer cells, **3** repressed the expression of cyclin E and the phosphorylation of CDK2, both of which are essential for G1/S transition.²¹ A more recent mechanistic study of **3** by Fukuoka et al. has further revealed that the compound disturbs the cell cycle progression at multiple points, including both G1/S and G2/M transitions, in human lung cancer cells.²² In this report using A549 and a **3**-resistant subline A549/ER, **3** was shown to inhibit pRb phosphorylation, to decrease the protein expression of cyclin A, cyclin B1, CDK2, and CDC2, and to suppress CDK2 catalytic activity with the induction of p53 and p21 proteins only in the parental A549 cells. All these observations indicate that this unique small molecule belongs to a novel class of cell cycle inhibitors.²³

Compound **3** displayed distinctive and promising antitumor profiles both in vitro and in vivo.²⁰ To assess the toxicity, the maximum tolerated dose (MTD), and the pharmacokinetics of this compound, phase I clinical trials have been conducted by the European Organization for Research and Treatment of Cancer (EORTC)—Early Clinical Studies Group (ECSG).^{24–27} In these studies, the major dose-limiting toxicity was determined to be myelosuppression, such as thrombocytopenia and neutropenia. Two partial responses with a more than 50% shrinkage of measurable tumors were observed in patients with uterine adenocarcinoma and breast cancer. In addition, disease stabilizations and some minor responses were also documented. Phase II trials are currently ongoing in Europe and the U.S. Other sulfonamide compounds examined herein were all synthesized by the procedures described earlier.^{14,18}

Results and Discussion

COMPARE Analysis. Compounds **2–8** were tested for in vitro antiproliferative activity against a panel of 39 human cancer cell lines in the DOS.¹¹ A 48 h assay with sulforhodamine B was employed for the evaluation.²⁸ Mean graphs⁴ of the compounds were prepared for the COMPARE algorithm based on the growth inhibition parameter of GI₅₀ (drug concentration required for 50% inhibition of cell proliferation). The log GI₅₀ (GI₅₀ in units of M) data are available as Supporting Information. In the NCI COMPARE analysis,⁴ a comparable mean graph signature can be seen among drugs with a common mode of action. Thus, **2** and **3** were used as seed compounds in COMPARE to

Table 1. COMPARE Analysis of a Series of Antitumor Sulfonamides^a

ranking order	compound	<i>r</i> ^b
(A) Based on the Mean Graph Fingerprint of 2		
1	4	0.861
2	5	0.718
3	Navelbine	0.652
4	Taxol	0.559
5	Vincristine	0.542
6	6	0.280
7	7	0.257
8	3	0.221
9	8	0.186
(B) Based on the Mean Graph Fingerprint of 3		
1	6	0.762
2	7	0.754
3	5	0.473
4	4	0.269
5	2	0.221
6	8	0.185

^a The mean graph fingerprints of **2** and **3** were individually compared with those of other test compounds using the COMPARE algorithm. The data on 200 standard drugs in the DOS were also included in the calculations, and the three drugs with correlation coefficients greater than 0.5 ($P < 0.001$) are presented here.

^b Pearson's correlation coefficient.

categorize our sulfonamide agents on the basis of their growth-inhibitory patterns. The calculation results are presented in Table 1, where compounds are ordered in accordance with Pearson's correlation coefficient. The mean graph signatures of **2** and **3** were also compared with those of more than 200 standard drugs in the DOS database. Among them, three drugs with correlation coefficients greater than 0.5 ($P < 0.001$) are included in Table 1.

Using **2** as an initial seed in COMPARE resulted in the identification of **4** and **5** as highly related to **2** with correlation coefficients greater than 0.7 (Table 1A). On the basis of the mean of log GI₅₀ values for 39 cell lines (MG-MID), **2** (MG-MID = -6.30) and **4** (MG-MID = -6.49) were equally active and **5** (MG-MID = -5.71) was slightly less active. Furthermore, the COMPARE run with the standard drugs assessed the top three **2**-related agents ($r > 0.5$) to be navelbine, taxol, and vincristine, all of which are well-known mitotic arrest agents. This result is consistent with the fact that **2** is an antimetabolic agent, although, strictly speaking, only taxol stabilizes microtubules. On the other hand, the mean graph signatures of **3** and **6–8** showed poor correlations ($r < 0.3$) compared with **2**, suggesting that all these agents are independent of anti-tubulin activity as exhibited by **2**. In light of the SAR study, the motif of *N*-(2-aminophenyl or 2-amino-3-pyridinyl)-4-methoxybenzenesulfonamide, which is common to **2**, **4**, and **5**, was regarded as a pharmacophore for a **2** type of microtubule-depolymerizing agent.

Another round of COMPARE using **3** as a seed revealed that **6** and **7** significantly correlated with **3** ($r > 0.7$), although the growth-inhibitory potency of **7** (MG-MID = -4.12) was rather low compared with those of **3** (MG-MID = -4.81) and **6** (MG-MID = -5.04) (Table 1B). A 3-chloro substituent on the indole moiety of this series may interact with a putative cellular target(s), leading to enhancement of the drug activity.¹⁸ Compound **8**, an amide analogue of **3**, was not only inferior (MG-MID = -4.44) but also unrelated ($r < 0.2$) to **3** with respect to the mean graph activity profile. These find-

ings indicated the *N*-(3-chloro-7-indolyl)benzenesulfonamide motif as a structural determinant for the activity pattern of the compound **3** class. However, compound **5**, possessing the same core structure, resembled **2** ($r = 0.718$) rather than **3** ($r = 0.473$) in the mean graph signature. The compound also contains the *N*-(2-aminophenyl)-4-methoxybenzenesulfonamide motif associated with the **2** type of antimetabolic activity, and thus, this core structure would appear to be the dominant pharmacophore for the activity profile of **5**. In the COMPARE analysis based on the mean graph fingerprint of **3**, there were no standard agents with correlation coefficients greater than 0.5. This supports the idea that **3** is a novel type of antiproliferative agent with a mechanism of action distinct from those of conventional anticancer drugs in clinical use.^{18,20}

Flow Cytometric Cell Cycle Analysis. To compare the effects of compounds **2–8** on cell cycle progression, fluorescence-activated cell sorter (FACS) analysis was performed with HCT116-C9 cells (Figure 1).²⁹ Cells were treated with each compound at 8 μ M for 12 h. Compound **3** alone was tested further at extended time points of 24, 36, and 48 h. In addition, the inhibitory activity of each compound on tubulin polymerization was measured (Table 2).

As expected from the COMPARE data, **4** and **5** caused a clear G2/M arrest like **2**. As shown in Table 2, all these compounds were capable of inhibiting tubulin polymerization with low micromolar IC₅₀ values. Furthermore, a marked increase in the mitotic index was observed microscopically in the cells treated with each of them for 12 h (data not shown). On the other hand, **6** led to a decrease of S and an increase of G2/M like **3**. The cell cycle effect of **7** was only marginal, corresponding to its lower activity compared with **3** and **6**. These three compounds did not increase the mitotic index at all after a 12 h treatment (data not shown), consistent with their insignificant activities against tubulin polymerization (IC₅₀ > 100 μ M). Hence, the drug-induced G2/M increase is considered to be due to cell cycle perturbation in the G2 phase. Compound **8**, inferior and unrelated to both **2** and **3** in its activity profile, showed almost negligible effects on the cell cycle progression of HCT116-C9 and on tubulin polymerization.

At the 12 h time point, no drugs produced the sub-G1 fraction indicative of programmed cell death (apoptosis),³⁰ suggesting that the conditions of drug treatment (at 8 μ M for 12 h) are suitable for microarray analysis to investigate early characteristic changes in gene expression. In the time course experiment, **3** caused a decrease of S and an increase of G2/M in a time-dependent manner, eventually resulting in the appearance of the sub-G1 fraction after 48 h of treatment. From the time point of 24 h, a drop in the early S fraction was also evident, indicating perturbation at the G1/S transition. This effect seems to be related to the G1-targeting action of **3** as reported previously in P388 murine leukemia^{18,20} and A549 human lung carcinoma cells.²²

High-Density Oligonucleotide Array Expression Analysis. To profile compounds **2–8** on the basis of their effects on gene expression, we used oligonucleotide microarray analysis with Affymetrix HuGene FL (Hu6800) arrays.^{12,29} HCT116-C9 cells were treated for

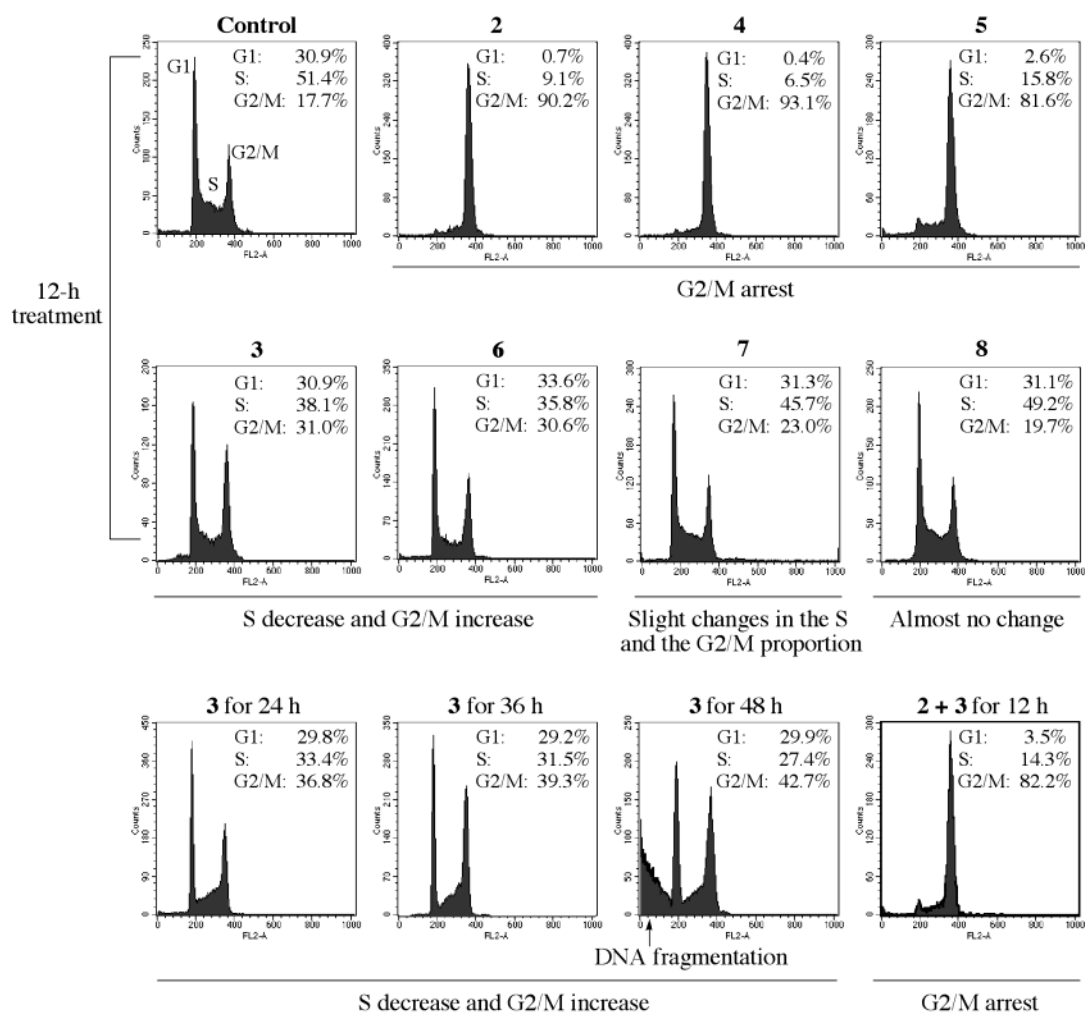


Figure 1. Flow cytometric cell cycle analysis. Drug effects on cell cycle progression of HCT116-C9 cells were examined according to the procedure described in Experimental Section. The experiment was performed in triplicate with each test compound, and representative DNA histograms are presented. The percentage of the cells in each cell cycle phase was calculated using the ModFit LT software for the FACSCalibur flow cytometer (Becton-Dickinson) to afford the mean of three independent data. Errors were within $\pm 10\%$ of the reported values.

Table 2. Inhibition of Tubulin Polymerization^a

compound	IC ₅₀ ^b (μ M)	compound	IC ₅₀ ^b (μ M)
2	2.2	6	>100
4	2.1	7	>100
5	9.5	8	>100
3	>100		

^a Microtubule assembly was evaluated turbidimetrically at 350 nm 30 min after the reaction mixture was warmed from 4 to 37 °C. The experiment was carried out in triplicate with each test compound. The IC₅₀ values were calculated using the least-squares method to afford the means of three independent experimental data. Errors were within $\pm 15\%$ of the reported values. ^b Drug concentration required for 50% inhibition of tubulin polymerization.

12 h with each compound at 8 μ M or with 0.015% DMSO (control). Listed in Table 3 (in Supporting Information) are genes up- or down-regulated at least 2-fold compared with control cells. The criteria for the gene selection are described in the table footnote.

Compound **2** treatment resulted in a 2-fold or more induction and repression of 22 and 9 transcripts, respectively. Of the 22 genes induced, 16 and 5 genes were also up-regulated by **4** and **5**, respectively, whereas only 2 genes were up-regulated by **3**. Because the induction of these two genes (i.e., tumor-associated

antigen GA733-1 and caveolin 1) was common to compounds **2–6** but not to the less active compounds **7** and **8**, it might be explained by nonspecific chemosensitivity of HCT116-C9 rather than by some specific mechanism of drug action. There was no overlap between the profiles of **2** and **3** as to the down-regulation of gene expression. Of the nine genes repressed by **2**, seven and five genes were also down-regulated by **4** and **5**, respectively. It should be noted that all three compounds significantly decreased the mRNA levels of two α -tubulin subtypes. The accumulation of tubulin monomers has been found to lead to the transcriptional repression of tubulin genes by a feedback regulatory mechanism.^{31,32} Therefore, we conclude that down-regulation of the α -tubulin transcripts is a common cellular response to the compound **2** class of microtubule-depolymerizing agents. Other common features of **2**, **4**, and **5** were seen in the induction of Cyr61, chondroitin sulfate proteoglycan 2, and clone 23933 and in the repression of Id-2 and DEAD-box protein p72. Judging from their synchronism in the three different drug treatments, it would appear that all of these expression changes, in addition to α -tubulin down-regulation, have some relevance to the antimitotic and

Table 4. Cell Growth Inhibition Assay Using **2**- and **3**-Resistant Cancer Cell Lines^a

compoundd	IC ₅₀ ^b (μM)			IC ₅₀ ^b (μM)		
	P388	P388/4.0r-M	RR ^c	HCT116-C9	HCT116-C9-C1	RR ^c
2	0.19	15	78	0.90	0.96	1.1
3	0.61	0.59	0.97	0.21	29	1.4 × 10 ²
5	1.2	1.2	1.0	0.37	2.2	5.9

^a Growth-inhibitory effects of **2**, **3**, and **5** were compared in the cell-based screen with P388, P388/4.0r-M (**2**-resistant), HCT116-C9, and HCT116-C9-C1 (**3**-resistant) cancer cell lines. The MTT assays were performed twice in triplicate with each test compound. The IC₅₀ values were calculated using the least-squares method to afford the means of six independent data. Errors were within ±15% of the reported values. ^b Drug concentration to inhibit cell proliferation by 50% relative to untreated control cells after 72 h of continuous drug exposure. ^c RR, relative resistance value, equals the IC₅₀ value for the resistant cell line divided by the IC₅₀ value for the parental cell line.

antitumor properties of the **2**-related agents. Interestingly, trimethoxystilbenes (i.e., combretastatins) and their analogues have been reported to be potent microtubule-depolymerizing agents that bind to the colchicine site as well.^{33–35} They have recently attracted a great deal of attention because of their promising in vivo antitumor efficacy and antivasular action.^{36,37} Microarray analysis to compare the transcriptional effects of these agents and **2** would also be of considerable interest.

Compound **3** treatment resulted in a 2-fold or more induction and repression of 18 and 163 genes, respectively. This dominant transcriptional repression seems to be characteristic of the expression profile of **3**. Of the total of 181 (=18 + 163) genes, 151 genes were also found in the array data for **6** (12 induced and 139 repressed), corresponding to the activity data based on the mean graph signature and the cell cycle effect. It is of particular interest that 118 genes were also found in the array data for **5** (12 induced and 106 repressed). This unexpected result reveals that **5** exhibits the **3**-type profile as well as the **2**-type profile on the gene expression basis, even though its activity fingerprint is similar to that of **2**. Compound **7**, a des-chloro derivative of **3**, significantly affected the expression of 10 genes (2 induced and 8 repressed), all of which were included in the genes altered by **3**. In this experimental setting, compound **8**, an amide analogue of **3**, did not change any transcript level 2-fold or more. With respect to the extent of the transcriptional effect, the array data for **3**, **7**, and **8** correlate well with the results of cell-based antitumor screens as described above.

In the compound **3** class, characteristic transcriptional alteration (mainly repression) was observed in sets and subsets of genes involved in cellular metabolism, cell cycle control, signal transduction, transcription, mRNA biogenesis, translation, immunomodulation, cell adhesion, proteolysis, cytoskeleton, and membrane trafficking. Among them, the down-regulation of subsets of genes regulating mitochondrial functions and energy metabolism implies cell cycle arrest at the G1/S checkpoint (termed the restriction point), where nutritive conditions are checked before committing to the DNA replication.¹⁸ In yeast, cell size is monitored at this point to determine whether sufficient nutrients are available to complete a full cell cycle. The transcriptional repression of several DNA replication-associated and mitosis-associated genes should also be noted because of its clear correlation with the cell cycle effect of **3**. Although the precise mode of action of **3** has not yet been fully understood, the microarray data shown here illuminate drug-sensitive cellular pathways suggestive of potential expression markers for the **3** type of antitumor activity.

By visiting the DTP web site (<http://dtp.nci.nih.gov>), one can see a variety of sulfonamide compounds possessing anticancer properties in the NCI60 activity database. Some of the sulfonamide agents are structurally related to **3** and may exhibit growth-inhibitory effects through metal chelation (e.g., NSC compounds 641105, 643599, 647959, 676553, 676569, 676571, 687773, 687776, 687778, 687779, and 687780) or carbonic anhydrase (CA) inhibition (the data for representative compounds are available in recent papers³⁸). From an examination, there seemed to be no significant correlation between any of these agents and **3** on the basis of their mean graph signatures. However, it is still possible that metal chelation and/or CA inhibition, at least in part, might be involved in the mode of antitumor action of **3**. To address this possibility, array-based transcription profiling of relevant compounds could be informative, since it proved to be powerful for revealing the **3**-type profile latent in **5**.

Cell-Based Assays To Verify the Bifunctional Profile of Compound 5. To provide further evidence that **5** interacts with both cellular targets of **2** and **3** as suggested by the gene expression data, we performed additional cell-based assays described below. According to our hypothesis, a mixture of **2** and **3** should be indistinguishable from **2** and **5** in cell cycle analysis. As expected, cotreatment of **2** (8 μM) and **3** (8 μM) for 12 h resulted in a clear G2/M arrest of HCT116-C9 cells, corresponding to the histogram data for **2** and **5** (Figure 1). This result indicates that the G2/M arrest phenotype is predominant over the **3**-like cell cycle phenotype in the FACS analysis of **5**.

We next compared growth-inhibitory effects of **2**, **3**, and **5** in the MTT assay³⁹ using P388 (parental), P388/4.0r-M¹⁵ (subclone resistant to **2**), HCT116-C9 (parental), and HCT116-C9-C1²⁹ (subclone resistant to **3**). On the IC₅₀ basis, the relative resistances of P388/4.0r-M and HCT116-C9-C1 to **2** and **3** were approximately 80- and 140-fold, respectively (Table 4). These two subclones showed no cross-resistance to other anticancer agents such as adriamycin, etoposide, mitomycin C, cisplatin, vincristine, and taxol (see ref 15 for P388/4.0r-M and unpublished data taken by our group for HCT116-C9). This suggests that their resistance mechanisms are unrelated to the overexpression of P-glycoprotein causing a multidrug-resistance phenotype. Importantly, **5** displayed unchanged antiproliferative potency against P388/4.0r-M (IC₅₀ = 1.2 μM) compared with the parental P388 (IC₅₀ = 1.2 μM). Although HCT116-C9-C1 showed a little cross-resistance to **5**, the relative resistance value of 5.9-fold was much less than the 140-fold to **3**. In addition, the IC₅₀ value of **5** toward this subclone was still at the low micromolar level (2.2 μM). These

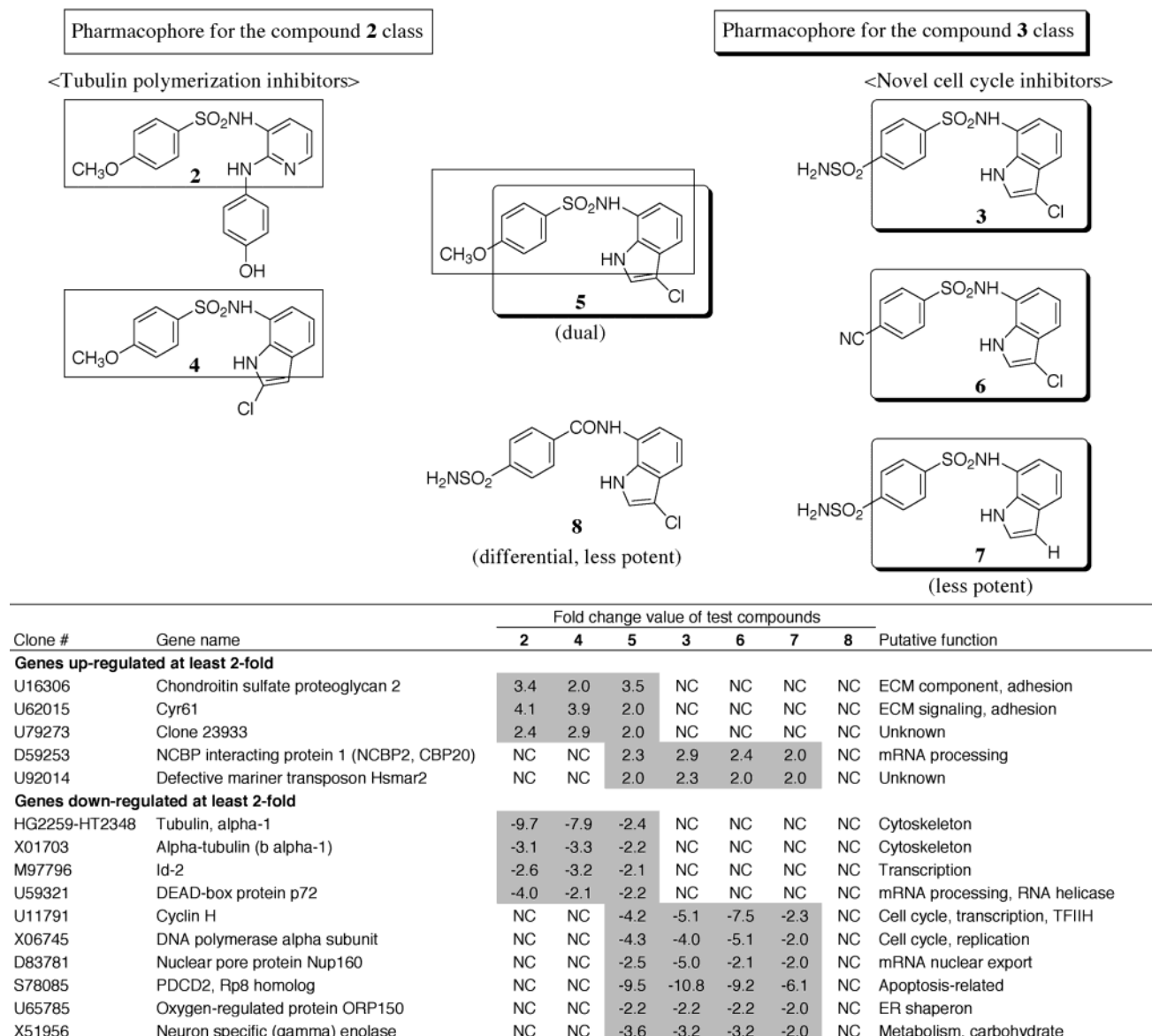


Figure 2. Summary of the structure and gene expression relationships of a series of antitumor sulfonamides.

observations support the idea that **5** is effective against the **2**-resistant P388/4.0r-M by interacting with a cellular target(s) of **3** and is also effective against **3**-resistant HCT116-C9-C1 by interacting with tubulin, a cellular target of **2**. Taken together, all of these results are very consistent with the microarray data, leading to a conclusion that **5** contains both antitumor profiles of **2** and **3**.

Structure and Gene Expression Relationship Study. Exploiting the human genome database has allowed the systematic construction of comprehensive assay screens such as kinase and G-protein-coupled receptor (GPCR) panels. High-throughput screening using these assay panels facilitates detailed profiling of biologically active small molecules on the basis of their activity patterns (phenotypic fingerprints). It is also possible to profile compounds in terms of their genome-wide expression patterns (transcriptional fingerprints) by using DNA microarray technology. Both of these sophisticated characterization methods for small-molecule collections are expected to be extremely useful for rationalizing drug discovery and development

programs. In particular, array-based transcription profiling of drug candidates will be increasingly in practical and common use to provide validity for continuing development. This is the basis for our work here to apply microarray analysis to clarify the structure and gene expression relationships of a series of antitumor sulfonamides.

The observed structure and gene expression relationships are summarized in Figure 2. The major findings are as follows: (i) The expression profile of the compound **2** class of agents can be attributed to the *N*-(2-aminophenyl or 2-amino-3-pyridinyl)-4-methoxybenzenesulfonamide motif based on the distinctive overlap among the array data for **2**, **4**, and **5**, including the repression of two α -tubulin subtypes. (ii) The dual character of **5**, which has the antitumor characteristics of both **2** and **3**, is evident in the array-based profiling. The compound **3**-like activity profile of this molecule was not seen clearly in the cell-based phenotypic screens using COMPARE and FACS analyses because of the predominant **2**-like activity profile. (iii) Significant overlap among the array data for **3**, **5**, and **6** indicates

that the 4 (para)-substituent on the phenyl moiety can be varied without greatly influencing the expression profile of the compound **3** class. (iv) Except for the induction of two genes (tumor-associated antigen GA733-1 and caveolin 1), there is no overlap between the array data for **3** and **4** possessing a 2-chloro substituent. This contrasts with the significant overlap between the array data for **3** and **5** possessing a 3-chloro substituent, suggesting that the 2-chloro substituent obstructs an interaction with a cellular target(s) of the compound **3** class. (v) Compared with **3**, an overlapped but very limited set of genes is affected by the des-chloro derivative **7**. From this observation and the SAR summary, it is conjectured that the 3-chloro substituent may be critically involved in the interaction between **3** and its molecular target(s). (vi) Because there are no genes for which the mRNA levels are changed at least 2-fold by **8**, the sulfonamide linkage between two aromatic rings is considered indispensable for the expression profile of the compound **3** class. This is consistent with the SAR summary. (vii) On the basis of points ii–vi, it can finally be concluded that the *N*-(3-chloro-7-indolyl)-benzenesulfonamide motif is an essential pharmacophore for the expression profile of the compound **3** class of antitumor agents.

Compound **3** has been evaluated in the phase I clinical setting, displaying antitumor activities including disease stabilization.^{24–27} An appropriate assessment of these clinical responses may require demonstration of the drug effects on the primary target molecule(s) or closely associated cellular pathways in cancer patients. In relation to this point, preclinical measurements of transcriptional changes in cancer cells (in vitro) or tumors (in vivo) in response to compound **3** treatment may provide potential expression markers indicative of the drug efficacy. We therefore tried to narrow down candidate genes implicated in compound **3** efficacy by applying the following procedures to all our array data: (i) eliminate genes also affected by structurally related compounds with different mechanisms of action, using the data for **2**, **4**, **8**, and **3**; (ii) select genes also affected by different compounds with substantially the same mechanism of action, using the data for **5–7** and **3**. Although **7** is less active than **3**, the fact that its mean graph signature is similar to that of **3** suggests that the compound still retains marginal ability to bind to a cellular target(s) of **3**. Thus, the array data for **7** were used to reduce the number of putatively relevant genes. In consequence, characteristic alterations in gene expression in response to the compound **3** class were observed in the induction of NCBP interacting protein 1 (NCBP2, CBP20) and defective mariner transposon Hsmar2 and in the repression of cyclin H, DNA polymerase α , nuclear pore protein Nup160, Rp8 homologue PDCD2, oxygen-regulated protein ORP150, and neuron-specific (γ) enolase. The transcriptional regulation of all these genes could be highly associated with the **3**-sensitive pathways, at least in HCT116-C9 cells.

Besides the chemical genomic approach⁴⁰ with a variety of compounds as described above, conventional approaches with different cancer species and varied drug concentrations have also been employed for identifying the genes most relevant to compound **3** efficacy. In such experiments, 0.8 μ M of **3** (12 h treatment), a

clinically achievable drug concentration, led to a 2-fold or more repression of nine genes in common in three different cancer cell lines, HCT116-C9 colon carcinoma, MDA-MB-435 breast carcinoma, and MOLT-4 leukemia. Importantly, these nine genes include DNA polymerase α , cyclin H, and Rp8 homologue PDCD2 (unpublished results of T. Owa, A. Yokoi, and T. Nagasu). The DNA polymerase α protein is an essential enzyme for DNA replication.⁴¹ The cyclin H protein forms part of the CDK-activating kinase (CAK) together with CDK7 and MAT1, playing a key role in coordinating cell cycle progression, transcription, and DNA repair.^{42–44} The significant down-regulation of these two genes correlates with the cell cycle perturbation caused by **3**. The precise function of PDCD2 is still unclear, although its rat homologue Rp8 is thought to be involved in apoptosis.⁴⁵ Further microarray analyses and target-finding studies of **3** are under way to establish the connection between the functions of a target molecule(s) and the downstream effects on gene expression. Such efforts (medicinal genomic approaches) should allow us to utilize all the above-mentioned expression changes by **3** as molecular biological endpoints for the pharmacodynamic assessment of drug efficacy. Moreover, given the clinical activity of **3**, new important targets for future molecular-based cancer therapeutics might be found among the genes affected profoundly by this interesting compound.

Conclusion

The microarray analysis presented herein has made it possible to characterize the compound **2** and compound **3** classes of antitumor sulfonamides on the basis of drug-induced changes in gene expression. The array data allowed us to identify the essential pharmacophore structure and drug-sensitive cellular pathways for each class. Furthermore, the dual character of **5**, which displays characteristics of both **2** and **3**, was revealed by array-based transcription profiling, even though the **3**-type profile of this molecule was not clear in cell-based phenotypic screens using the COMPARE analysis and cell cycle monitoring. In conclusion, these results provide an example of the potential benefits of structure and gene expression relationship studies in medicinal genomics.

Experimental Section

General. All commercial solvents and reagents were used without further purification. Reactions were generally conducted under a nitrogen atmosphere using magnetic stirring. Analytical thin-layer chromatography (TLC) was performed on silica gel plates (Merck, No. 5715). Merck silica gel 60 (230–400 mesh) was used for the flash chromatographic purification of some compounds. Compounds **2**, **3**, **5**, and **6** were synthesized using procedures reported previously^{13,18} and characterized by obtaining spectroscopic and analytical data as described earlier.^{13,18} The other new derivatives **4**, **7**, and **8** were characterized according to the following general methods. Melting points were determined on a Yanagimoto micromelting point apparatus and are reported uncorrected. Proton (¹H) NMR spectra were obtained at 400 MHz on a Varian UNITY 400 spectrometer in DMSO-*d*₆. Chemical shifts are expressed in δ (ppm) units relative to tetramethylsilane (TMS) reference. Mass spectra (FABMS) were recorded on a JEOL JMS-SX102AQQ using a direct introduction method in the FAB+ ion mode. Elemental analyses (C, H, N) were carried out at the Eisai Analytical Chemistry Section, and the results were within $\pm 0.4\%$ of the theoretical values.

N-(2-Chloro-7-indolyl)-4-methoxybenzenesulfonamide (4). To a solution of 2-chloro-7-nitroindole⁴⁶ (460 mg, 2.34 mmol) in 2-propanol (8 mL) were added Fe powder (392 mg, 7.02 mmol) and an aqueous solution (1.6 mL) of NH₄Cl (25 mg, 0.467 mmol). After the mixture was stirred at 60 °C for 2 h, activated charcoal (ca. 200 mg) was added to the reaction mixture. The insoluble materials were filtered off and washed with EtOAc (20 mL), followed by the immediate addition of 4-methoxybenzenesulfonyl chloride (484 mg, 2.34 mmol) and pyridine (0.76 mL, 9.40 mmol). The reaction mixture was stirred at room temperature for 3 h, diluted with EtOAc, and washed successively with 0.5 N aqueous HCl, H₂O, saturated aqueous NaHCO₃, and brine. The organic layer was dried over anhydrous MgSO₄, filtered, and concentrated under reduced pressure. Purification by flash chromatography (eluted EtOAc–hexane) gave **4** (652 mg, 83%) as a white solid: melting point 150–152 °C (after recrystallization from EtOAc–hexane); ¹H NMR (400 MHz, DMSO-*d*₆) δ 3.78 (3H, s), 6.43 (1H, s), 6.74 (1H, dd, *J* = 7.7, 0.92 Hz), 6.86 (1H, dd, *J* = 7.9, 7.7 Hz), 7.00–7.05 (2H, AA'BB'), 7.21 (1H, dd, *J* = 7.9, 0.92 Hz), 7.65–7.70 (2H, AA'BB'), 9.52 (1H, br s), 11.48 (1H, br s); MS (FAB+) *m/z* 336 (M⁺). Anal. (C₁₅H₁₃N₃O₃SCl) C, H, N.

N-(7-Indolyl)-1,4-benzenedisulfonamide (7). A solution of 7-nitroindole (2.74 g, 16.9 mmol) in MeOH (75 mL) was hydrogenated over 10% palladium on carbon (270 mg) under H₂ at 1 atm overnight. The catalyst was filtered off, and the filtrate was evaporated to give almost pure 7-aminoindole. The amine product was immediately dissolved in EtOAc (50 mL) and pyridine (2.8 mL, 34.6 mmol) and then reacted with 4-sulfamoylbenzenesulfonyl chloride⁴⁷ (4.32 g, 16.9 mmol) at room temperature for 5 h. The reaction mixture was diluted with EtOAc and washed successively with 0.5 N aqueous HCl, H₂O, saturated aqueous NaHCO₃, and brine. The organic layer was dried over anhydrous MgSO₄, filtered, and concentrated under reduced pressure. Purification by flash chromatography (eluted with EtOAc–hexane) gave **7** (5.08 g, 86%) as a white solid: melting point 218–219 °C (after recrystallization from EtOH–hexane); ¹H NMR (400 MHz, DMSO-*d*₆) δ 6.41 (1H, dd, *J* = 3.1, 2.0 Hz), 6.68 (1H, dd, *J* = 7.7, 0.92 Hz), 6.83 (1H, dd, *J* = 7.7, 7.9 Hz), 7.31 (1H, d, *J* = 3.1 Hz), 7.33 (1H, dd, *J* = 7.9, 0.92 Hz), 7.56 (2H, br s), 7.93 (4H, s), 10.16 (1H, br), 10.80 (1H, br s); MS (FAB+) *m/z* 351 (M⁺). Anal. (C₁₄H₁₃N₃O₄S₂) C, H, N.

N-(3-Chloro-7-indolyl)-4-sulfamoylbenzamide (8). To a solution of 3-chloro-7-nitroindole¹⁸ (1.50 g, 7.63 mmol) in 2-propanol (20 mL) were added Fe powder (1.28 g, 22.9 mmol) and an aqueous solution (4 mL) of NH₄Cl (82 mg, 1.53 mmol). After the mixture was stirred at 60 °C for 2 h, activated charcoal (ca. 500 mg) was added to the reaction mixture. The insoluble materials were filtered off and washed with EtOAc (200 mL). The obtained organic layer was washed with saturated aqueous NaHCO₃ and brine, dried over anhydrous MgSO₄, filtered, and concentrated under reduced pressure to give almost pure 7-amino-3-chloroindole as a grayish-brown solid. The amine product was immediately dissolved in THF (20 mL), and then 4-sulfamoylbenzoic acid (1.54 g, 7.65 mmol) and 1,1'-carbonyldiimidazole (1.36 g, 8.39 mmol) were added to the solution. After being stirred under reflux overnight, the reaction mixture was diluted with EtOAc and washed successively with 0.5 N aqueous HCl, H₂O, saturated aqueous NaHCO₃, and brine. The organic layer was dried over anhydrous MgSO₄, filtered, and concentrated under reduced pressure. Purification by flash chromatography (eluted with EtOAc–hexane) gave **7** (1.89 g, 71%) as a white solid: melting point 280–281.5 °C (after recrystallization from EtOH–hexane); ¹H NMR (400 MHz, DMSO-*d*₆) δ 7.14 (1H, dd, *J* = 7.9, 7.7 Hz), 7.38 (1H, dd, *J* = 7.9, 0.92 Hz), 7.41 (1H, dd, *J* = 7.7, 0.92 Hz), 7.56 (2H, br s), 7.56 (1H, s), 7.95–8.01 (2H, AA'BB'), 8.16–8.22 (2H, AA'BB'), 10.39 (1H, br), 11.24 (1H, br s); MS (FAB+) *m/z* 349 (M⁺). Anal. (C₁₅H₁₂N₃O₃SCl) C, H, N.

Human Cancer Cell Line Panel, Cell Growth Inhibition Assay, and Data Analysis. Characterization of 39 human cancer cell lines of the DOS has been described elsewhere:¹¹ breast cancer (HBC-4, BSY-1, HBC-5, MCF-7, and

MDA-MB-231); brain tumor (U251, SF-268, SF-295, SF-539, SNB-75, and SNB-78); colon cancer (HCC2998, KM-12, HT-29, HCT15, and HCT116); lung cancer (NCI-H23, NCI-H226, NCI-H522, NCI-H460, A549, DMS273, and DMS114); melanoma (LOX-IMVD); ovarian cancer (OVCAR-3, OVCAR-4, OVCAR-5, OVCAR-8, and SK-OV-3); renal cancer (RXF-631L and ACHN); stomach cancer (St-4, MKN1, MKN7, MKN28, MKN45, and MKN74); prostate cancer (DU-145 and PC-3). All of these cell lines were grown in RPMI 1640 supplemented with 5% fetal bovine serum, penicillin (100 units/mL), and streptomycin (100 μg/mL) at 37 °C in humidified air containing 5% CO₂. Measurements of cell growth inhibition and data calculations were performed according to the reported methods.^{4,11} The sulforhodamine B assay²⁸ with 48 h drug exposure was employed for the chemosensitivity screen in the DOS. Drug concentrations with 10-fold dilution ranging from 100 μM to 10 nM were tested in the assay. The main measure of chemosensitivity used in the database and calculations of Pearson's correlation coefficients was GI₅₀ (drug concentration that inhibits cell proliferation by 50% relative to untreated control cells).

Cell Cloning and Culture. HCT116 human colon carcinoma was purchased from American Type Culture Collection (Manassas, VA). HCT116-C9 was isolated as a 3-sensitive subclone from the parental HCT116 cell line by using a limiting dilution method.²⁹ This cell line was used for flow cytometry and oligonucleotide microarray analyses. HCT116-C9-C1, a 3-resistant subclone, was obtained from a viable colony of HCT116-C9 after continuous drug exposure with serial dose escalation of **3**.²⁹ P388 murine leukemia was supplied by the Cancer Chemotherapy Center, Japan Foundation for Cancer Research (Tokyo, Japan). P388/4.0r-M, a 2-resistant subclone, was established at Tsukuba Research Laboratories, Eisai Co., Ltd.¹⁵ HCT116-C9 and HCT116-C9-C1 were maintained in RPMI 1640 medium containing 10% fetal bovine serum, penicillin (100 units/mL), and streptomycin (100 μg/mL) at 37 °C in humidified air containing 5% CO₂. For the culture of P388 and P388/4.0r-M, mercaptoethanol (5 × 10⁻² mM) and sodium pyruvate (1 mM) were added to the medium as supplements. All of these cell lines were used for cell growth inhibition assays with 3-(4,5-dimethylthiazol-2-yl)-2,5-diphenyltetrazolium bromide (MTT).³⁹

Flow Cytometric Cell Cycle Analysis.²⁹ Exponentially growing HCT116-C9 cells were seeded in six-well plates (4.5 × 10⁵ cells/well) and precultured for 1 day. Test compounds (2.0 mM stock solution in DMSO) were added to the plates at the final concentration of 8 μM, and incubation was continued for 12 h. Compound **3** was further tested at extended time points of 24, 36, and 48 h to examine the time course of its cell cycle effect. The combination effect of **2** and **3** on cell cycle progression was also investigated at the 12 h time point. For fluorescence-activated cell sorter (FACS) analysis, the cells were fixed in 70% ethanol, treated with RNase (1 mg/mL), and stained with propidium iodide (50 μg/mL). The DNA content was quantified by detecting red fluorescence with a flow cytometer (FACSCalibur, Becton-Dickinson). Data analysis was done with CellQuest and ModFit LT software (Becton-Dickinson). The experiment was carried out in triplicate for each analysis.

Tubulin Polymerization Assay.^{15,18} Test compounds dissolved at graded concentrations in DMSO were added to the wells of 96-well microtiter plates containing 1 mg/mL microtubule protein from bovine brain. A final DMSO concentration of 5% (v/v) and compound concentrations of 0.30, 1.0, 3.0, 10, 30, and 100 μM were used for assays in polymerization buffer (0.1 M 2-(*N*-morpholino)ethanesulfonic acid, 1 mM EGTA, 0.5 mM MgCl₂, pH 6.8). After 30 min of incubation at 4 °C, the mixture was warmed to 37 °C with 1 mM GTP to start tubulin polymerization. Microtubule assembly was monitored by measuring the turbidity kinetically at 350 nm with a microplate reader (THERMO max, Molecular Devices) for 40 min. At the time point of 30 min, the polymerization of the control reached a plateau level. Therefore, the turbidity at 30 min was plotted on a linear scale versus the concentration of the test compound

on a log scale. The experiment was carried out in triplicate for each compound, and the drug concentration causing 50% inhibition of polymerization was determined by the least-squares method.

High-Density Oligonucleotide Array Expression Analysis.²⁹ HCT116-C9 cells were plated at 5.0×10^6 cells/dish in 10 cm diameter dishes with 10 mL of fresh medium. After 24 h of preincubation, the cells were treated for 12 h with each test compound at 8 μ M or with 0.015% DMSO (control). Sample preparation was performed according to established protocols.¹² In brief, total RNA was extracted from the cells using Trizol (GIBCO BRL) and further purified with RNeasy columns (Qiagen). Double-stranded cDNA was prepared from 10 μ g of total RNA using the SuperScript Choice System (GIBCO BRL) and T7-d(T)₂₄ primers. The cDNA product was purified by phenol–chloroform extraction. In vitro transcription was carried out with an RNA transcript labeling kit containing biotinylated UTP and CTP (Enzo Diagnostics). After purification with RNeasy columns, the cRNA was fragmented and then hybridized to Affymetrix GeneChip HuGene FL (Hu6800) arrays. According to the EukGE-WS2 protocol, the probe arrays were washed and stained with streptavidin–phycoerythrin and biotinylated goat antistreptavidin on an Affymetrix fluidics station. Fluorescence intensities were captured with a Hewlett-Packard confocal laser scanner. All quantitative data were processed using the Affymetrix GeneChip software.¹² Up- or down-regulated genes were selected according to the criteria as described in the legend to Table 3 (Supporting Information).

Cell Growth Inhibition Assay Using Compound 2 Resistant and Compound 3 Resistant Cancer Cell Lines. P388/4.0r-M¹⁵ and HCT116-C9-C1²⁹ were used as subclonal cell lines resistant to **2** and **3**, respectively. P388 and P388/4.0r-M cells were seeded at 1.25×10^3 cells/well in 96-well round-bottomed plates, and HCT116-C9 and HCT116-C9-C1 cells were seeded at 3.0×10^3 cells/well in 96-well flat-bottomed plates. Compounds **2**, **3**, and **5** were dissolved at 20 mM in DMSO and further diluted with the culture medium (see Cell Cloning and Culture above) to prepare 3-fold serial dilutions with the maximum concentration being 100 μ M after the addition into each well. After 24 h of preincubation, the obtained dilutions were added to the plates and then incubation was continued for 3 days. The antiproliferative activity (IC₅₀ value) was determined by the MTT colorimetric method.³⁹ The assays were performed twice in triplicate with each test compound. Relative resistance (RR) values were calculated as the IC₅₀ values for the resistant cell line divided by the IC₅₀ values for the parental cell line.

Acknowledgment. We thank Dr. J. Kuromitsu and Dr. T. Kawai for their helpful discussions and assistance with the microarray analysis. Mass spectra and elemental analysis data were kindly provided by the Eisai Analytical Chemistry Section.

Supporting Information Available: The log GI₅₀ (GI₅₀ in units of M) data for compounds **2–8** in the DOS panel of 39 human cancer cell lines and Table 3 presenting the full details of gene expression data for the same test compounds. This material is available free of charge via the Internet at <http://pubs.acs.org>.

References

- Lander, E. S.; Linton, L. M.; Birren, B.; Nusbaum, C.; Zody, M. C.; et al. Initial sequencing and analysis of the human genome. *Nature* **2001**, *409*, 860–921.
- Venter, J. C.; Adams, M. D.; Myers, E. W.; Li, P. W.; Mural, R. J.; et al. The sequence of the human genome. *Science* **2001**, *291*, 1304–1351.
- Scherf, U.; Ross, D. T.; Waltham, M.; Smith, L. H.; Lee, J. K.; et al. A gene expression database for the molecular pharmacology of cancer. *Nat. Genet.* **2000**, *24*, 236–244.
- (a) Paull, K. D.; Shoemaker, R. H.; Hodes, L.; Monks, A.; Scudiero, D. A.; et al. Display and analysis of patterns of differential activity of drugs against human tumor cell lines: development of mean graph and COMPARE algorithm. *J. Natl. Cancer Inst.* **1989**, *81*, 1088–1092. (b) Monks, A.; Scudiero, D.; Skehan, P.; Shoemaker, R.; Paull, K.; et al. Feasibility of a high-flux anticancer drug screen using a diverse panel of cultured human tumor cell lines. *J. Natl. Cancer Inst.* **1991**, *83*, 757–766.
- Ramaswamy, S.; Tamayo, P.; Rifkin, R.; Mukherjee, S.; Yeang, C. H.; et al. Multiclass cancer diagnosis using tumor gene expression signatures. *Proc. Natl. Acad. Sci. U.S.A.* **2001**, *98*, 15149–15154.
- Su, A. I.; Welsh, J. B.; Sapinoso, L. M.; Kern, S. G.; Dimitrov, P.; et al. Molecular classification of human carcinomas by use of gene expression signatures. *Cancer Res.* **2001**, *61*, 7388–7393.
- Zimmermann, J.; Erdmann, D.; Lalande, I.; Grossenbacher, R.; Noorani, M.; et al. Proteasome inhibitor induced gene expression profiles reveal overexpression of transcriptional regulators ATF3, GADD153 and MAD1. *Oncogene* **2000**, *19*, 2913–2920.
- Kudoh, K.; Ramanna, M.; Ravatn, R.; Elkahloun, A. G.; Bittner, M. L.; et al. Monitoring the expression profiles of doxorubicin-induced and doxorubicin-resistant cancer cells by cDNA microarray. *Cancer Res.* **2000**, *60*, 4161–4166.
- Martinez, E. J.; Corey, E. J.; Owa, T. Antitumor activity- and gene expression-based profiling of ecteinascidin Et 743 and phthalascidin Pt 650. *Chem. Biol.* **2001**, *8*, 1151–1160.
- Rabow, A. A.; Shoemaker, R. H.; Sausville, E. A.; Covell, D. G. Mining the National Cancer Institute's tumor-screening database: identification of compounds with similar cellular activities. *J. Med. Chem.* **2002**, *45*, 818–840.
- (a) Dan, S.; Tsunoda, T.; Kitahara, O.; Yanagawa, R.; Zembutsu, H.; et al. An integrated database of chemosensitivity to 55 anticancer drugs and gene expression profiles of 39 human cancer cell lines. *Cancer Res.* **2002**, *62*, 1139–1147. (b) Yamori, T.; Matsunaga, A.; Sato, S.; Yamazaki, K.; Komi, A.; et al. Potent antitumor activity of MS-247, a novel DNA minor groove binder, evaluated by an in vitro and in vivo human cancer cell line panel. *Cancer Res.* **1999**, *59*, 4042–4049. (c) Naasani, I.; Seimiya, H.; Yamori, T.; Tsuruo, T. FJ5002: a potent telomerase inhibitor identified by exploiting the disease-oriented screening program with COMPARE analysis. *Cancer Res.* **1999**, *59*, 4004–4011.
- Lockhart, D. J.; Dong, H.; Byrne, M. C.; Follettie, M. T.; Gallo, M. V.; et al. Expression monitoring by hybridization to high-density oligonucleotide arrays. *Nat. Biotechnol.* **1996**, *14*, 1675–1680.
- Yoshino, H.; Ueda, N.; Nijima, J.; Sugumi, H.; Kotake, Y.; et al. Novel sulfonamides as potential, systemically active antitumor agents. *J. Med. Chem.* **1992**, *35*, 2496–2497.
- Owa, T.; Okauchi, T.; Yoshimatsu, K.; Sugi, N. H.; Ozawa, Y.; et al. A focused compound library of novel *N*-(7-indolyl)benzenesulfonamides for the discovery of potent cell cycle inhibitors. *Bioorg. Med. Chem. Lett.* **2000**, *10*, 1223–1226.
- Yoshimatsu, K.; Yamaguchi, A.; Yoshino, H.; Koyanagi, N.; Kitoh, K. Mechanism of action of E7010: inhibition of mitosis by binding to the colchicine site of tubulin. *Cancer Res.* **1997**, *57*, 3208–3213.
- Koyanagi, N.; Nagasu, T.; Fujita, F.; Watanabe, T.; Tsukahara, K.; et al. In vivo tumor growth inhibition produced by a novel sulfonamide, E7010, against rodent and human tumors. *Cancer Res.* **1994**, *54*, 1702–1706.
- Yamamoto, K.; Noda, K.; Yoshimura, A.; Fukuoka, M.; Furuse, K.; et al. Phase I study of E7010. *Cancer Chemother. Pharmacol.* **1998**, *42*, 127–134.
- Owa, T.; Yoshino, H.; Okauchi, T.; Yoshimatsu, K.; Ozawa, Y.; et al. Discovery of novel antitumor sulfonamides targeting G1 phase of the cell cycle. *J. Med. Chem.* **1999**, *42*, 3789–3799.
- Owa, T.; Nagasu, T. Novel sulphonamide derivatives for the treatment of cancer. *Expert Opin. Ther. Pat.* **2000**, *10*, 1725–1740.
- Ozawa, Y.; Sugi, N. H.; Nagasu, T.; Owa, T.; Watanabe, T.; et al. E7070, a novel sulfonamide agent with potent antitumor activity in vitro and in vivo. *Eur. J. Cancer* **2001**, *37*, 2275–2282.
- Watanabe, T.; Sugi, N.; Ozawa, Y.; Owa, T.; Nagasu, T.; et al. A novel antitumor agent ER-35744, targeting G1 phase. III. Studies of mechanism of action. *Proc. Am. Assoc. Cancer Res.* **1996**, *37*, A2667, 391.
- Fukuoka, K.; Usuda, J.; Iwamoto, Y.; Fukumoto, H.; Nakamura, T.; et al. Mechanism of action of the novel sulfonamide anticancer agent E7070 on cell cycle progression in human non-small cell lung cancer cells. *Invest. New Drugs* **2001**, *19*, 219–227.
- Owa, T.; Yoshino, H.; Yoshimatsu, K.; Nagasu, T. Cell cycle regulation in the G1 phase: a promising target for the development of new chemotherapeutic anticancer agents. *Curr. Med. Chem.* **2001**, *8*, 1487–1503.
- Dittrich, C.; Dumez, H.; Calvert, H.; Hanauske, A. R.; Ravic, M.; et al. Phase I and pharmacokinetic study of E7070 in patients with solid tumors as single iv infusion, weekly $\times 4$, q 6 weeks. *Proc. Am. Assoc. Cancer Res.* **2000**, *41*, A3875, 609.

- (25) Droz, J. P.; Roche, H.; Zanetta, S.; Terret, C.; Blay, J. Y.; et al. Phase I trial of five-days continuous infusion E7070 [*N*-(3-chloro-7-indolyl)-1,4-benzenedisulfonamide] in patients (pts) with solid tumors. *Proc. Am. Assoc. Cancer Res.* **2000**, *41*, A3876, 609.
- (26) (a) Punt, C. J. A.; Fumoleau, P.; Walle, B. V. D.; Deporte-Fety, R.; Bourcier, C.; et al. Phase I and pharmacokinetic (PK) study of E7070, a novel sulphonamide, given daily \times 5 every 3 weeks as a 1-hour intravenous infusion in patients (pts) with advanced solid tumors. *Proc. Am. Assoc. Cancer Res.* **2000**, *41*, A3877, 609. (b) Punt, C. J.; Fumoleau, P.; van de Walle, B.; Faber, M. N.; Ravic, M.; et al. Phase I and pharmacokinetic study of E7070, a novel sulfonamide, given at a daily times five schedule in patients with solid tumors. A study by the EORTC-early clinical studies group (ECSG). *Ann. Oncol.* **2001**, *12*, 1289–1293.
- (27) Raymond, E.; ten Bokkel-Huinink, W. W.; Taieb, J.; Beijnen, J. H.; Mekhaldi, S.; et al. Phase I and pharmacokinetic (PK) study of E7070, a new chloroindolylsulfonamide, given as a 1-hour infusion every 3 weeks in patients (pts) with advanced solid tumors. *Proc. Am. Assoc. Cancer Res.* **2000**, *41*, A3889, 611.
- (28) Skehan, P.; Storeng, R.; Scudiero, D.; Monks, A.; McMahon, J.; et al. New colorimetric cytotoxicity assay for anticancer-drug screening. *J. Natl. Cancer Inst.* **1990**, *82*, 1107–1112.
- (29) Yokoi, A.; Kuromitsu, J.; Kawai, T.; Nagasu, T.; Sugi, N. H.; et al. Profiling novel sulfonamide antitumor agents with cell-based phenotypic screens and array-based gene expression analysis. *Mol. Cancer Ther.* **2002**, *1*, 275–286.
- (30) Rödicker, F.; Stiewe, T.; Zimmermann, S.; Pützer, B. M. Therapeutic efficacy of E2F1 in pancreatic cancer correlates with *TP73* induction. *Cancer Res.* **2001**, *61*, 7052–7055.
- (31) Ben-Ze'ev, A.; Farmer, S. R.; Penman, S. Mechanisms of regulating tubulin synthesis in cultured mammalian cells. *Cell* **1979**, *17*, 319–325.
- (32) Rosania, G. R.; Chang, Y.-T.; Perez, O.; Sutherland, D.; Dong, H.; et al. Myoseverin, a microtubule-binding molecule with novel cellular effects. *Nat. Biotechnol.* **2000**, *18*, 304–308.
- (33) Pettit, G. R.; Rhodes, M. R. Antineoplastic agents 389. New syntheses of the combretastatin A-4 prodrug. *Anticancer Drug Des.* **1998**, *13*, 183–191.
- (34) Ohsumi, K.; Nakagawa, R.; Fukuda, Y.; Hatanaka, T.; Morinaga, Y.; et al. Novel combretastatin analogues effective against murine solid tumors: design and structure–activity relationships. *J. Med. Chem.* **1998**, *41*, 3022–3032.
- (35) Wang, L.; Woods, K. W.; Li, Q.; Barr, K. J.; McCroskey, R. W.; et al. Potent, orally active heterocycle-based combretastatin A-4 analogues: synthesis, structure–activity relationship, pharmacokinetics, and in vivo antitumor activity evaluation. *J. Med. Chem.* **2002**, *45*, 1697–1711.
- (36) Adams, J.; Elliott, P. J. New agents in cancer clinical trials. *Oncogene* **2000**, *19*, 6687–6692.
- (37) Beauregard, D. A.; Hill, S. A.; Chaplin, D. J.; Brindle, K. M. The susceptibility of tumors to the antivascular drug combretastatin A4 phosphate correlates with vascular permeability. *Cancer Res.* **2001**, *61*, 6811–6815.
- (38) (a) Supuran, C. T.; Scozzafava, A. Carbonic anhydrase inhibitors and their therapeutic potential. *Expert Opin. Ther. Pat.* **2000**, *10*, 575–600. (b) Scozzafava, A.; Supuran, C. T. Carbonic anhydrase inhibitors: Synthesis of *N*-morpholyl-thiocarbonyl-sulfonylamino aromatic/heterocyclic sulfonamides and their interaction with isozymes I, II and IV. *Bioorg. Med. Chem. Lett.* **2000**, *10*, 1117–1120. (c) Supuran, C. T.; Briganti, F.; Tilli, S.; Chegwidan, W. R.; Scozzafava, A. Carbonic anhydrase inhibitors: sulfonamides as antitumor agents? *Bioorg. Med. Chem.* **2001**, *9*, 703–714.
- (39) Mosmann, T. Rapid colorimetric assay for cellular growth and survival: application to proliferation and cytotoxicity assays. *J. Immunol. Methods* **1983**, *65*, 55–63.
- (40) Stockwell, B. R.; Hardwick, J. S.; Tong, J. K.; Schreiber, S. L. Chemical genetic and genomic approaches reveal a role for copper in specific gene activation. *J. Am. Chem. Soc.* **1999**, *121*, 10662–10663.
- (41) Foiani, M.; Lucchini, G.; Plevani, P. The DNA polymerase alpha-primase complex couples DNA replication, cell-cycle progression and DNA damage response. *Trends Biochem. Sci.* **1997**, *22*, 424–427.
- (42) Nigg, E. A. Cyclin-dependent kinase 7: at the cross-roads of transcription, DNA repair and cell cycle control? *Curr. Opin. Cell Biol.* **1996**, *8*, 312–317.
- (43) Yankulov, K. Y.; Bentley, D. L. Regulation of CDK7 substrate specificity by MAT1 and TFIIF. *EMBO J.* **1997**, *16*, 1638–1646.
- (44) Araujo, S. J.; Tirode, F.; Coin, F.; Pospiech, H.; Syvaaja, J. E.; et al. Nucleotide excision repair of DNA with recombinant human proteins: definition of the minimal set of factors, active forms of TFIIF, and modulation by CAK. *Genes Dev.* **2000**, *14*, 349–359.
- (45) Kawakami, T.; Furukawa, Y.; Sudo, K.; Saito, H.; Takami, S.; et al. Isolation and mapping of a human gene (PDCD2) that is highly homologous to Rp8, a rat gene associated with programmed cell death. *Cytogenet. Cell Genet.* **1995**, *71*, 41–43.
- (46) Nakashima, T.; Suzuki, I. Ring contraction of 3-hydroxyquinolines to oxindoles with hydrogen peroxide in acetic acid. *Chem. Pharm. Bull.* **1969**, *17*, 2293–2298.
- (47) Holland, G. F.; Funderburk, W. H.; Finger, K. F. Preparation and anticonvulsant activity of *N*-substituted benzenedisulfonamides. *J. Med. Chem.* **1963**, *6*, 307–312.

JM0201060